

Morphological and structural evolution during thermally physical vapor phase growth of PbI_2 polycrystalline thin films



Hui Sun*, Xinghua Zhu, Dingyu Yang, Jun Yang, Xiuying Gao, Xu Li

College of Optoelectronic Technology, Chengdu University of Information Technology, NO. 24, Block 1, Xuefu Road, Chengdu 610225, PR China

ARTICLE INFO

Article history:

Received 19 March 2014

Received in revised form

6 July 2014

Accepted 23 July 2014

Communicated by: D.W. Shaw

Available online 1 August 2014

Keywords:

A1. Atomic force microscopy

A1. Growth models

A3. Physical vapor deposition processes

A3. Polycrystalline deposition

B2. Semiconducting lead compounds

ABSTRACT

PbI_2 polycrystalline thin films have been prepared by using a thermally physical vapor phase growth in vacuum. X-ray diffraction measurement and atomic force microscope analysis show that the structural change of the films occurs depending on growth condition. The width of the Urbach tail of the films indicates that the disordered structure inside the grains changes relying on preparation condition. It is found that the structure of the films is sensitive to growth parameter. A microstructure evolution model with respect to grain orientation is developed to explain the morphological and structural variation process during the films growth.

© 2014 Elsevier B.V. All rights reserved.

1. Introduction

Lead iodide (PbI_2) is a potential semiconductor material for ionizing radiation detection and digital X-ray imaging [1,2]. This material has a wide band gap ($E_g > 2.3$ eV) and high resistivity of about 10^{13} Ω cm reducing the dark current for detector application. Its high atomic weight ($Z_{\text{Pb}}=82$, $Z_{\text{I}}=53$) results in strong absorption of X-ray photons [3]. The relatively low melting point (about 406 °C) allows a thermal evaporation technique to be employed to grow polycrystalline films on indium–tin–oxide layer coated (ITO) glass and thin film transistor (TFT) array substrates. The structure of PbI_2 grains is hexagonal crystals with layered construction, which is the same as the structure of CdI_2 [4]. However, a great variability occurs in grain size, orientation and film density during the film growth depending on the process conditions. Ideally, PbI_2 grains stack together with layer-by-layer pattern as crystallographic c -axis perpendicular to substrate surface and depending upon deposition rate and temperature can largely maintain this orientation to a thickness of about 20 μm [5]. Once beyond this point, orientation becomes more varied. The past studies mainly focused on high source temperature mostly above 200 °C, and obvious temperature difference (more than 40 °C) between source and substrate [5–7]. We have performed a series of evaporation experiments with low source temperature

from 80 to 170 °C in a high vacuum environment 10^{-4} – 10^{-5} Pa. It was found that 140 °C (± 1 °C) source temperature is a critical point for PbI_2 source material sublimation from solid phase transforming to vapor phase. But not any film growth occurred on the substrate at this source temperature and lower substrate temperature. Also the situations in which the low source temperature (below 200 °C) and small temperature difference (5–10 °C) has not been noticed and studied. In this paper, we explored the structure sensitivity and the evolution mechanism of morphology and structure of the PbI_2 polycrystalline thin films grown by using thermally physical vapor phase growth at the low source temperature and small temperature difference between source and substrate.

2. Methods

PbI_2 thin films were grown in vacuum at a fixed source–substrate distance with different source–substrate temperature and deposition time, as shown in Table 1. Commercial PbI_2 powder (Sinopharm Chemical Reagent Co., Ltd., 99.9%) washed with distilled water and dried in vacuum for 10 h at 0.1 Pa and 60 °C. Then the dried powder was purified using a repeated sublimation purification technique in a sealed and evacuated quartz ampoule [8]. The glass substrates (Corning 7059) were cleaned by acetone and ethanol with ultrasonic vibration, washed repeatedly with deionized water, and finally dried by high purity argon (99.9992%) gas flow. The films growth was performed in a vacuum chamber

* Corresponding author. Tel.: 86 28 85966385.

E-mail address: sunhui@cuit.edu.cn (H. Sun).

Table 1
Experiment parameters for PbI_2 polycrystalline thin films growth.

| Sample | $T_{\text{sou}}(^{\circ}\text{C})$ | $T_{\text{sub}}(^{\circ}\text{C})$ | $t_{\text{dep}}(\text{h})$ | Film thickness (nm) |
|--------|------------------------------------|------------------------------------|----------------------------|---------------------|
| A | 150 | 145 | 0.3 | 303 (± 5) |
| B | 150 | 145 | 1.0 | 482 (± 5) |
| C | 160 | 155 | 0.3 | 673 (± 5) |
| D | 160 | 155 | 1.0 | 788 (± 5) |
| E | 170 | 165 | 0.3 | 959 (± 5) |
| F | 170 | 165 | 1.0 | 1231 (± 5) |

T_{sou} : source temperature, T_{sub} : substrate temperature, t_{dep} : deposition time.

with the pressure 10^{-4} Pa. The temperature of source and substrate was controlled by two separate Shimaden FP93 program controllers ($\pm 1^{\circ}\text{C}$ accuracy). The starting material was heated from 150 to 170°C . The films were deposited on substrates at various temperatures ranging from 145 to 165°C . The distance of source to substrate was 50 mm fixed. The grown films were labelled as A to F, depending on the growth condition as shown in Table 1.

The surface morphology of the as-grown PbI_2 films was investigated by a CSPM5000 atomic force microscope (AFM) with CSPM image process software. X-ray diffraction (XRD) was

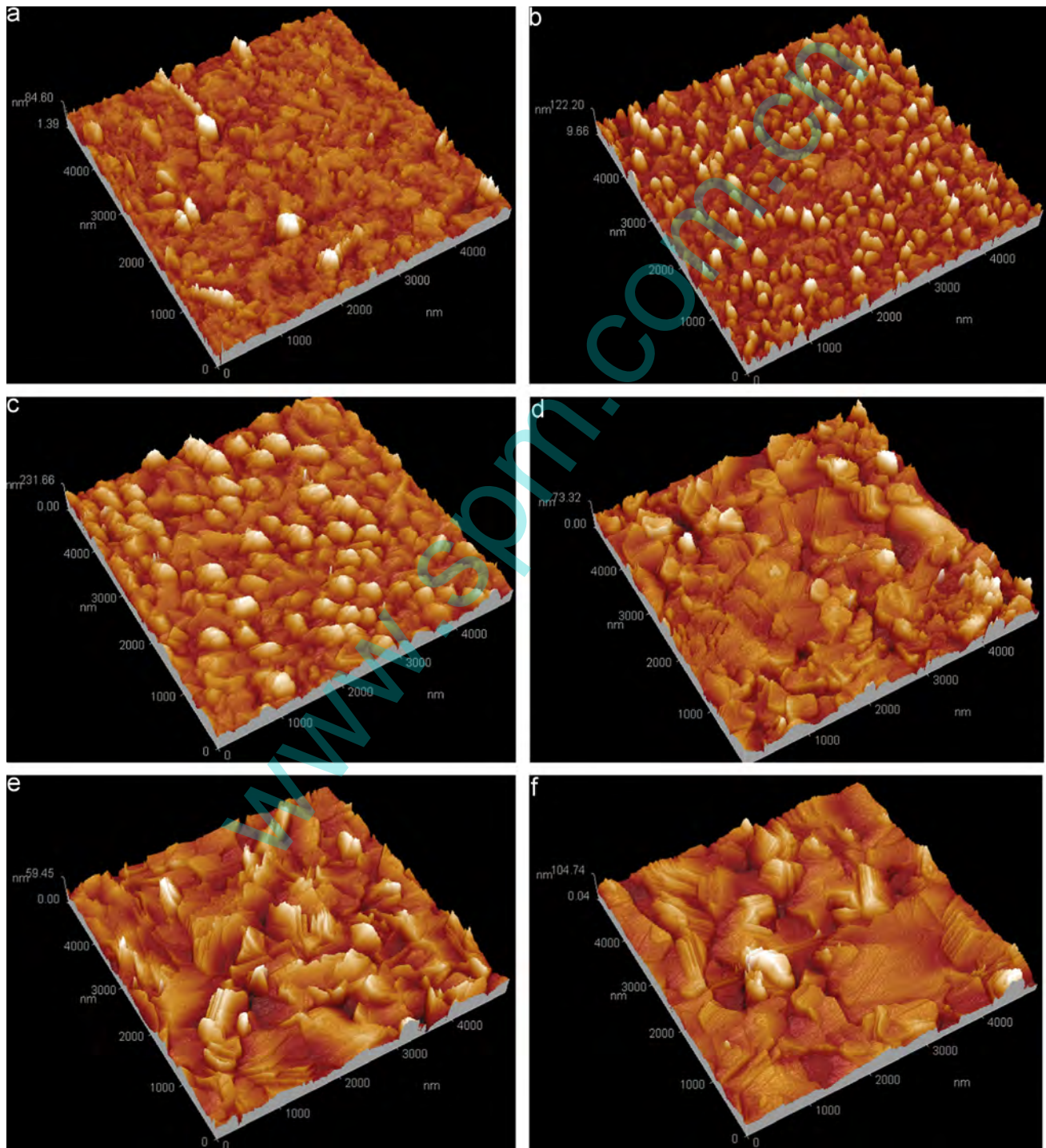


Fig. 1. AFM micrographs obtained by tapping mode of the PbI_2 thin films deposited on glass substrates. The label a to f is in line with the samples A to F in Table 1.

performed using a DX-2500 Cu K α radiation (1.54 Å, 30 kV, 20 mA) to analyze the film structure. The scanning angle was varied from 10° to 85° with steps of 0.03°. The film thickness was obtained by a Veeco Dektak 150 surface profiler. The optical absorption spectrum of the as-grown PbI₂ films as a function of wavelength was measured using a SHIMADZU UV2550 UV–vis spectrophotometer (200–900 nm).

3. Results and discussion

Fig. 1 shows AFM micrographs of the top view of the as-deposited PbI₂ films. Fig. 1(a and b) shows the PbI₂ films grown at $T_{\text{sou}}=150\text{ }^{\circ}\text{C}$, $T_{\text{sub}}=145\text{ }^{\circ}\text{C}$, with deposition time 0.3 h (a) and 1.0 h (b). The disordered structure of the both films is obtained under the two growth conditions, which is constituted of irregular shape grain or microcrystal, while a large grain is obtained with a long deposition time (1.0 h) compared to that with a short deposition time (0.3 h). The films shown in Fig. 1(c and d) were prepared at $T_{\text{sou}}=160\text{ }^{\circ}\text{C}$ and $T_{\text{sub}}=155\text{ }^{\circ}\text{C}$, also the grain size is larger under longer growth time. However, the regular shape grain gradually forms, especially the hexagonal shaped grain forming in films under $t_{\text{dep}}=1.0\text{ h}$. The as-deposited films with a dense structure and integrally hexagonal shaped grain were obtained at $T_{\text{sou}}=170\text{ }^{\circ}\text{C}$ and $T_{\text{sub}}=165\text{ }^{\circ}\text{C}$, as shown in Fig. 1(e and f). Both kinds of films show a more complete grain appearance, denser structure and higher crystalline degree under longer growth time and higher source and substrate temperature. Also it is found that the films are composed of hexagonal shaped grain with partial layers paralleled to the substrate plane, or forming an angle between the grains and substrate. It means that the grain orientation or arrangement mode is sensitive to growth conditions. This kind of growth characteristics was also observed with the substrate temperature from 180 to 210 °C [7].

Surface roughness average of the as-grown films can be obtained from the CSPM image software analysis, as demonstrated in Fig. 2. The results show that the roughness is in the range from 7 to 11 nm to the films prepared with 1.0 h growth time, which is smaller than that with 0.3 h (3–14 nm). For the films prepared at $T_{\text{sou}}=150\text{ }^{\circ}\text{C}$ and $T_{\text{sub}}=145\text{ }^{\circ}\text{C}$, the short growth time leads to a small surface roughness (about 5 nm), which also presents the

same result in the films prepared at $T_{\text{sou}}=170\text{ }^{\circ}\text{C}$ and $T_{\text{sub}}=165\text{ }^{\circ}\text{C}$. However, an opposite result was obtained in the films grown at $T_{\text{sou}}=160\text{ }^{\circ}\text{C}$ and $T_{\text{sub}}=155\text{ }^{\circ}\text{C}$. The low roughness occurs at the long deposition time. The variation of surface roughness mainly attributes to the structural change of the films. The opposite variation of the roughness derives from the configuration between the hexagonal grain and the substrate plane. The evaporation rate is small at a low source temperature which could cause a little bit of vapor condensing on the substrate surface and forming amorphous crystal nucleus without specific appearance. Meanwhile, these crystal nuclei are unstable which will re-evaporate from the substrate. The nuclei become larger following the higher temperature and longer deposition time, as shown in Fig. 1(a, b and c). It is worth noting that the grains with hexagonal appearance form at $T_{\text{sou}}=160\text{ }^{\circ}\text{C}$, $T_{\text{sub}}=155\text{ }^{\circ}\text{C}$ and $t_{\text{dep}}=1.0\text{ h}$ as well as the grains start to incline the *c*-axis toward the substrate plane, as shown in Fig. 1(d). Then the grain remains its hexagonal shape and enlarges its size under higher growth temperature and longer deposition time. And the surface will become smooth with small roughness.

Fig. 3(a) presents XRD spectra of the as-grown PbI₂ films for structural characterization. The peaks corresponding to (001), (002), (003) and (004) plane are identified from the Joint Committee on Powder Diffraction Standards (JCPDS, data no. 07-0235), which indicate that the as-grown PbI₂ films are 2H hexagonal structure with space group $P\bar{3}m1$ [9]. The peaks for samples A, B and C are not clear enough due to the very intensive (001) peak for samples D, E and F in the same coordinate system. The intensity of (001) peak for the films strengthen with increasing of growth temperature and deposition time, which also well meets the results from AFM observation.

An intensive peak, mostly the (001) peak, is observed from the XRD spectra indicating that the films are highly textured. Therefore, the as-grown films demonstrate a preferred orientation in the (001) plane that is in [001] crystal direction in the hexagonal crystal system and exactly perpendicular to the crystal *c*-axis. The degree of orientation in the direction (001) was found by estimating the texture coefficient $tc(hkl)$ by using [7,10]:

$$tc(hkl) = \frac{I(hkl)/I_0(hkl)}{[\sum I(hkl)/I_0(hkl)]/N} \quad (1)$$

where $I(hkl)$ is the measured peak intensity, $I_0(hkl)$ is the JCPDS data peak intensity for powder diffraction, and N is the number of measured peaks. The texture coefficient (tc) of (001) plane is shown in Fig. 3(b). The formation of the preferred orientation is related to the growth time, which can be defined by the residence time of the vapor particles for lattice adjusting. The orientation can occur at various planes with short deposition time, yet along with the prolongation of the deposition time, some planes were weakened and some planes were enhanced.

An evolution mechanism can be introduced to explain the change of films' morphology and structure, as shown in Fig. 4. Film growth begins with crystallographic *c*-axis oriented perpendicular to substrate plane in the in-plane mode [5,7]. The growth occurs mainly through constructing covalent monolayer of I–Pb–I and building of new monolayer in *c*-axis direction via van der Waals bonding [7], as shown with Type #1 in Fig. 4. The crystal *c*-axis is parallel to the normal of the substrate plane (*c'*). New growth centers or nuclei may form on the surface of monolayer after the change of conditions and then the monolayer becomes the substrate for new nuclei growth. Generally, it should obtain better film if the new nuclei grow at the same material surface, which is similar to homogeneity epitaxial. However, it is difficult to maintain orientation for growing thick films even if the growth conditions remain the same. The new nuclei can grow further as well as through building up covalent I–Pb–I monolayer, while the orientation becomes varied. This will cause the grain arranging as

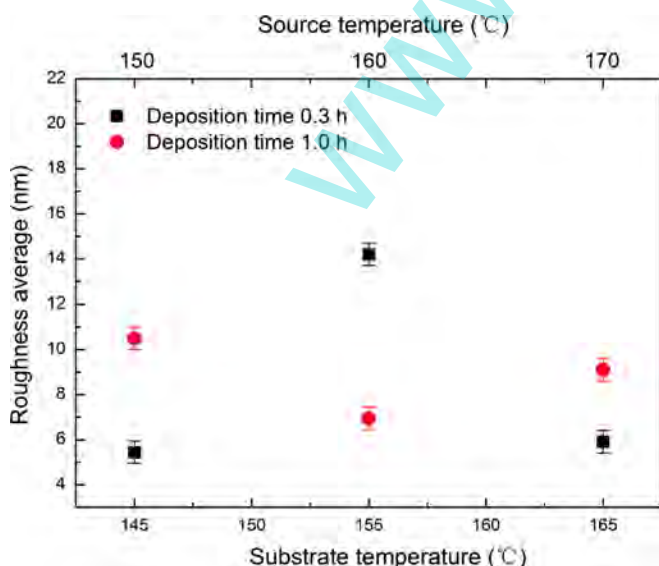


Fig. 2. Roughness average of the as-grown PbI₂ films versus growth temperature under different deposition times.

Type #2 or Type #3 which are shown in Fig. 4. From the AFM and XRD analysis, growth of the PbI_2 films is in agreement with this evolution mechanism. Most of the films construct as Type #2 (typically for sample E) or a mixture of Type #2 and Type #3 (typically for samples D and F). Schieber [7] had also presented

that the PbI_2 films grew as Type #1 to Type #3 along with the substrate temperature from 130 to 210 °C. The difference is that the film first constructed as Type #3 at lower growth temperature 130 °C, and Type #1 at 160 °C, then a mixture of Type #2 and Type #3 at 210 °C. An effective method named close spaced vapor

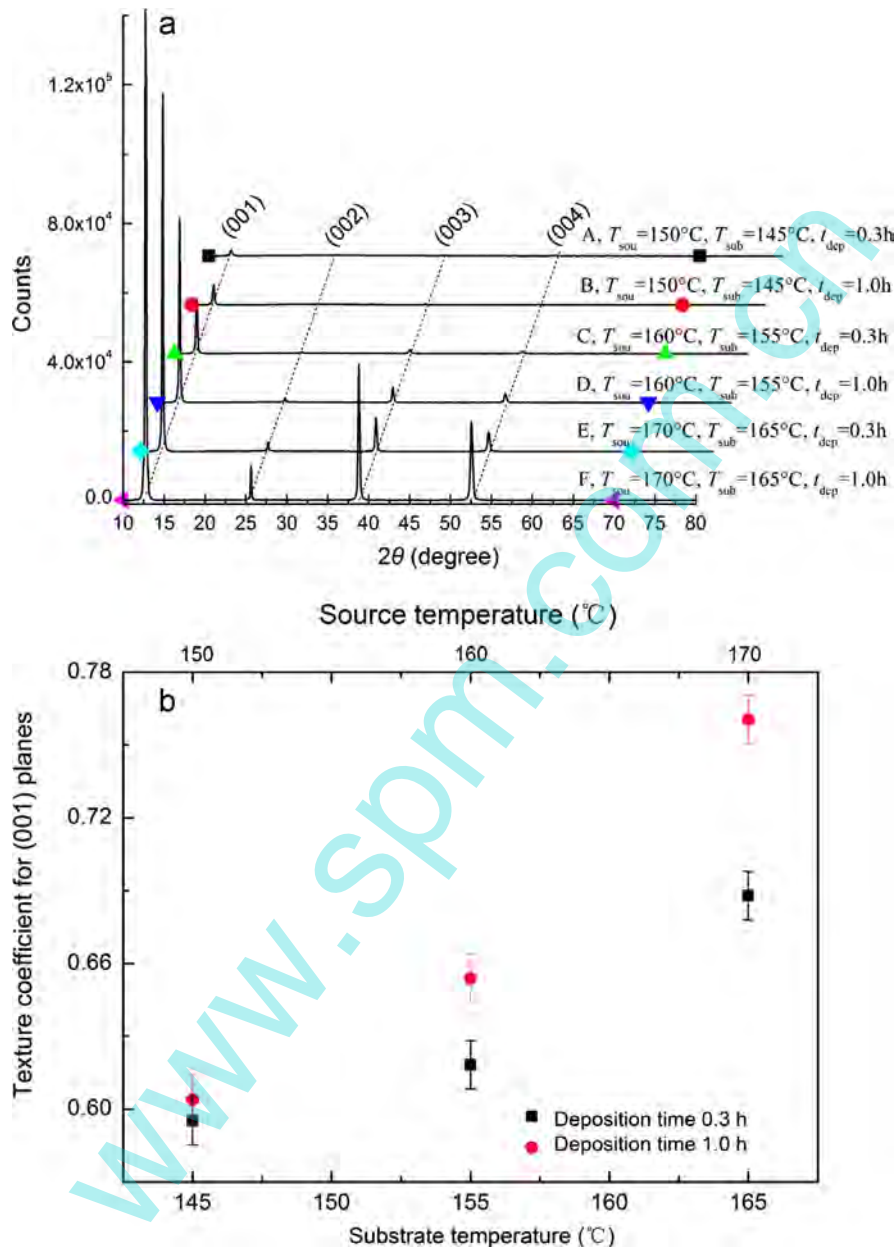


Fig. 3. (a) X-ray diffraction spectra of PbI_2 films deposited on glass substrate under various growth conditions. The label A to F is in line with the sample type in Table 1. (b) Texture coefficient for (001) crystal plane obtained from XRD data versus substrate and source temperature.

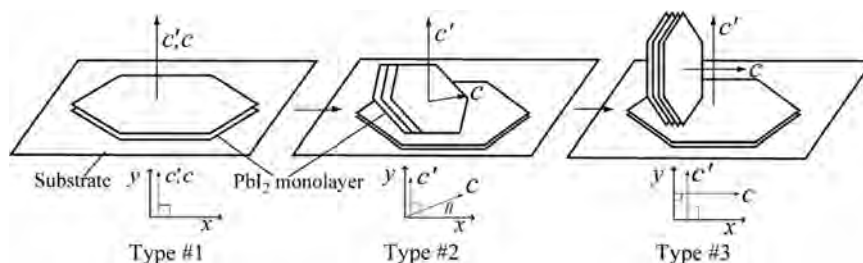


Fig. 4. Schematic representation of structural evolution for the growth of PbI_2 polycrystalline thin films.

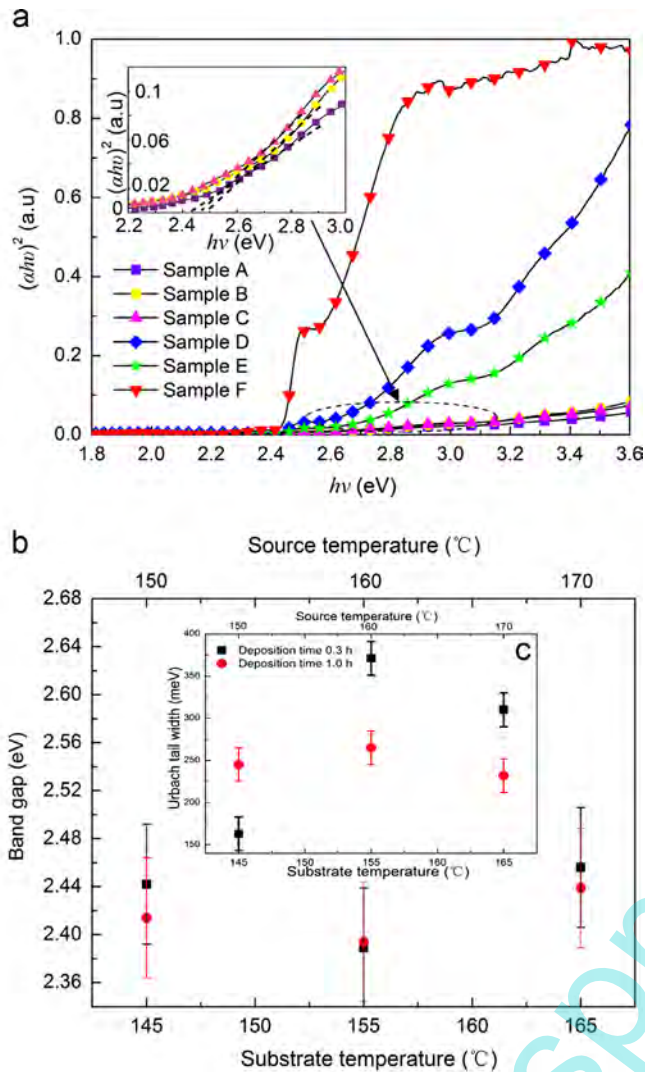


Fig. 5. (a) $(\alpha hv)^2$ versus $h\nu$ plot of the as-grown PbI_2 films. The label A to F is in line with the sample in Table 1. Band gap (b) and Urbach tail width (c) of the films versus substrate and source temperature.

deposition (CSVD) has been developed to obtain the PbI_2 films as only Type #3 mode [11].

The value of band gap was obtained from Tauc relation combined with optical absorption spectra [12,13]:

$$(\alpha hv) = A(hv - E_g)^{1/2} \quad (2)$$

where α , $h\nu$, E_g , and A are absorption coefficient, incident photon energy, band gap and constant, respectively. The band gap was determined by extrapolating the linear portion of the $(\alpha hv)^2$ versus $h\nu$ plots, as shown in Fig. 5(a). The E_g values were obtained from the intercept on $h\nu$ axis $(\alpha hv)^2=0$. Fig. 5(b) shows the plotting of the band gap versus growth temperature without remarkable variation of the band gap to the films deposited at different process conditions. The band gap of the film is closely related to the microstructure and stoichiometric proportion. The width of band tail localized states of the film can be decreased at a high substrate temperature, which can increase the band gap. Meanwhile, the evaporation, transport, deposition and re-evaporation processes lead to the loss of iodine (I), which can diminish the band gap.

The absorption behavior can be observed near the intrinsic absorption edge from an accurate evaluation of absorption curve,

which possibly originates from lattice defect (or imperfection of grains) leading to deep defect levels near the valence band top. The absorption presents an apparent trailing phenomenon which is the so-called Urbach tail [14]. Generally, it is thought that the band tail near the bottom of the conduction band, which generated from the disordered structure, is responsible for the Urbach tail width (E_u), resulting in an extension in the low energy zone. The disordered structure can produce tail localized states and the width is related to the density of the disordered state. The density of the disordered state of the film can be qualitatively analyzed with the tail width. The exponential relation between absorption coefficient (α) of the Urbach tail and photon energy $h\nu$ is represented by the following formula [14,15]:

$$\ln \alpha(\nu) = \frac{h\nu}{E_u} + C, \quad (3)$$

It can be obtained by plotting the logarithm of the absorption coefficient (α) versus $h\nu$ and taking the inverse of the slope ($1/\text{slope}$) from the linear part of the curve. The plotting of Urbach tail width versus growth temperature is shown in Fig. 5(c). It demonstrates that the smaller tail width accompanies the longer deposition time and higher growth temperature, which could reduce the density of the disordered state and increase the integrity of grains. This result corresponds to the analysis results obtained from AFM and XRD.

4. Conclusion

PbI_2 polycrystalline thin films have been prepared by using thermally physical vapor phase growth. Atomic force microscope studies indicate that the films consist of hexagonal grains with partial monolayer parallel to the substrate or portion to form an angle between (001) plane and substrate plane. X-ray diffraction analysis reveals that the as-grown PbI_2 films have a hexagonal structure and demonstrated preferred orientation along (00 l) ($l=1, 2, 3, \text{ and } 4$) planes. Both AFM and XRD show that the structure of the films is sensitive to growth condition. An evolution model is developed to explain the structural variation process with respect to the grain orientation impacting the morphology and structure of the as-grown films. The values of Urbach tail width indicate that the density of disordered structure results from the non-integrity of crystalline grain which could be reduced by increasing the growth temperature and time.

Acknowledgments

This work was supported by the National Natural Science Foundation of China No. 50902012, Scientific Research Foundation of CUIT No. CSRF201005, Scientific Research Fund of Sichuan Provincial Education Department No. 10ZA131, Technology Support Program Fund of Science and Technology Department of Sichuan Province No. 2014GZ0020, and Strategic Emerging Products Project Fund of Sichuan Province No. 2014GZX0012.

References

- [1] J.C. Lund, K.S. Shah, M.R. Squillante, F. Sinclair, IEEE Trans. Nucl. Sci. 35 (1988) 89.
- [2] K.S. Shah, J.C. Lund, F. Olschner, P. Bennett, J. Zhang, L.P. Moy, M.R. Squillante, Nucl. Instrum. Methods A 353 (1994) 85.
- [3] J.H. Hubbell, S.M. Seltzer, Tables of X-Ray Mass Attenuation Coefficients and Mass Energy-Absorption Coefficients from 1 keV to 20 MeV for Elements $Z=1$ to 92 and 48 Additional Substances of Dosimetric Interest, National Institute of Standards and Technology, USA, 1996.
- [4] P.A. Beckmann, Cryst. Res. Technol. 45 (2010) 455.

- [5] P.R. Bennett, K.S. Shah, Y. Dmitriev, M. Klugerman, T. Gupta, M. Squillante, R. Street, L. Partain, G. Zentai, R. Pavlyuchova, Nucl. Instrum. Methods A 505 (2003) 269.
- [6] M.R. Tubbs, A.J. Forty, J. Chem. Solids 26 (1985) 711.
- [7] M. Schieber, N. Zamoshchik, O. Khakhan, A. Zuck, J. Cryst. Growth 310 (2008) 3168.
- [8] H. Sun, X.H. Zhu, D.Y. Yang, Z.Y. He, S.F. Zhu, B.J. Zhao, J. Semicond. 33 (2012) 053002.
- [9] X.H. Zhu, Z.R. Wei, Y.R. Jin, A.P. Xiang, Cryst. Res. Technol. 42 (2007) 456.
- [10] B.D. Cullity, S.R. Stock, Elements of X-ray Diffraction, third ed., Prentice Hall, New Jersey, 2001.
- [11] X.H. Zhu, H. Sun, D.Y. Yang, X.L. Zheng, Nucl. Instrum. Methods A 691 (2012) 10.
- [12] J. Tauc, Amorphous and Liquid Semiconductors, Plenum Press, London and New York, 1974.
- [13] T. Ghosh, S. Bandyopadhyay, K.K. Roy, S. Kar, A.K. Lahiri, A.K. Maiti, K. Goswami, Cryst. Res. Technol. 43 (2008) 959.
- [14] F. Urbach, Phys. Rev. 92 (1953) 1324.
- [15] R.A. Street, Hydrogenated Amorphous Silicon, Cambridge University Press, Cambridge, 1991.

www.spm.com.cn